Chapter 1

Deuteron Spin and Magnetic Moment

1.1 Nuclear spin and parity: careful definitions

The binding energy of the deuteron fixes the radial scale of a central NN well, under the assumption that the relative orbital angular momentum is $\ell = 0$. That assumption must now be tested with every other measured property of the ground state: the total angular momentum (nuclear spin), the parity, and the magnetic dipole moment [6, 2].

1.1.1 What "nuclear spin" means

Each nucleon carries orbital angular momentum $\boldsymbol{\ell}$ and intrinsic spin $\boldsymbol{s} = \frac{1}{2}\hbar$ (in units where we often set $\hbar = 1$ for quantum numbers). Their sum is

$$\boldsymbol{j} = \boldsymbol{\ell} + \boldsymbol{s}. \tag{1.1}$$

In a nucleus the total angular momentum is the vector sum of all nucleon contributions. Nuclear physicists call this total $\boldsymbol{I}$ and name it the **nuclear spin**, even though it includes orbital motion as well as spin. The usual quantum rules apply:

$$\boldsymbol{I}^2 \to I(I+1)\hbar^2, \qquad I_z \to M_I\hbar, \quad M_I = -I, \ldots, +I. \tag{1.2}$$

When two angular momenta j_1 and j_2 are coupled, the allowed total values follow the triangle rule

$$J = |j_1 - j_2|, \, |j_1 - j_2| + 1, \ldots, \, j_1 + j_2. \tag{1.3}$$

This rule will be applied twice: first $\boldsymbol{S} = \boldsymbol{s}_p + \boldsymbol{s}_n$, then $\boldsymbol{I} = \boldsymbol{L} + \boldsymbol{S}$.

1.1.2 Parity

Parity is the behaviour of the spatial wave function under $\boldsymbol{r} \to -\boldsymbol{r}$. If $\psi(-\boldsymbol{r}) = +\psi(\boldsymbol{r})$ the parity is even ($\pi = +$); if $\psi(-\boldsymbol{r}) = -\psi(\boldsymbol{r})$ it is odd ($\pi = -$). A central-potential wave function separates as

$$\psi_{\ell m}(\boldsymbol{r}) = R_\ell(r) Y_{\ell m}(\theta, \phi). \tag{1.4}$$

Inversion leaves $r = |\boldsymbol{r}|$ unchanged but sends $(\theta, \phi) \to (\pi - \theta, \phi + \pi)$. Spherical harmonics obey

$$Y_{\ell m}(\pi - \theta, \phi + \pi) = (-1)^\ell Y_{\ell m}(\theta, \phi). \tag{1.5}$$

Therefore

$$\psi_{\ell m}(-\boldsymbol{r}) = (-1)^\ell \psi_{\ell m}(\boldsymbol{r}), \qquad \pi = (-1)^\ell. \tag{1.6}$$

Even ℓ gives even parity; odd ℓ gives odd parity.

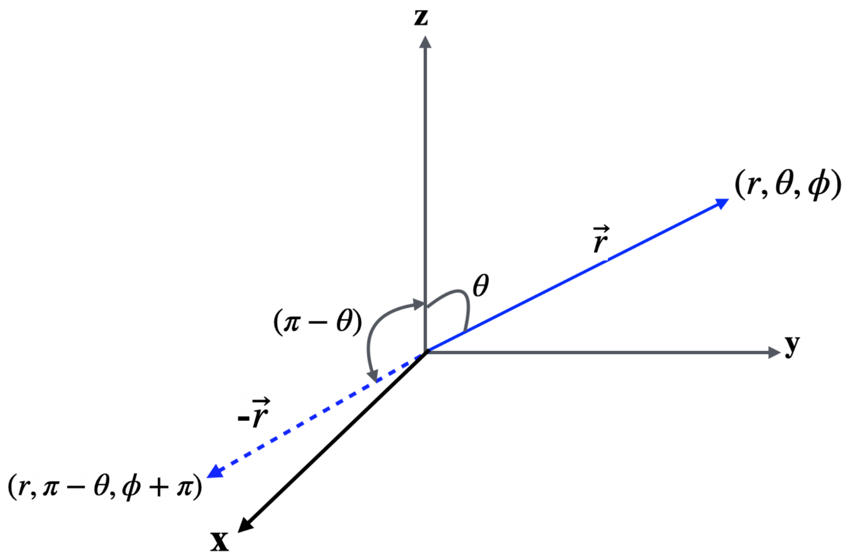

Figure 1.1: Inversion $\boldsymbol{r} \leftrightarrow -\boldsymbol{r}$. Nuclear states have definite parity when the Hamiltonian conserves parity.

1.1.3 Experimental assignment for the deuteron

Experiment gives

$$I^\pi(^2\mathrm{H}) = 1^+. \tag{1.7}$$

That single label will eliminate most of the angular-momentum possibilities we might have imagined.

1.2 Coupling two spins: four ways to make $I = 1$

The deuteron total angular momentum is

$$\boldsymbol{I} = \boldsymbol{s}_p + \boldsymbol{s}_n + \boldsymbol{L}, \tag{1.8}$$

where $\boldsymbol{L}$ is the relative orbital angular momentum. Each nucleon has $s = \frac{1}{2}$, so the total spin $\boldsymbol{S} = \boldsymbol{s}_p + \boldsymbol{s}_n$ obeys

$$S = \left|\tfrac{1}{2} - \tfrac{1}{2}\right|, \ldots, \tfrac{1}{2} + \tfrac{1}{2} = 0,\ 1. \tag{1.9}$$

For fixed S and L, the second application of Equation (1.3) gives

$$|L - S| \leq I \leq L + S. \tag{1.10}$$

We require $I = 1$:

- If $S = 0$, then $I = L$, so only $L = 1$ works.
- If $S = 1$, then $|L - 1| \leq 1 \leq L + 1$, which permits $L = 0, 1, 2$.

Thus there are exactly four couplings [6]:

(a) spins parallel ($S = 1$) with $L = 0$;

(b) spins antiparallel ($S = 0$) with $L = 1$;

(c) spins parallel ($S = 1$) with $L = 1$;

(d) spins parallel ($S = 1$) with $L = 2$.

Parity decides among them. The deuteron has *even* parity, and orbital parity is $(-1)^L$. Therefore L must be even: $L = 1$ is ruled out. Cases (b) and (c) drop. We are left with

$$^3S_1 \quad (L = 0,\, S = 1) \qquad \text{and} \qquad ^3D_1 \quad (L = 2,\, S = 1). \tag{1.11}$$

The bound state is **100% spin triplet**. There is no bound singlet pn state.

The notation $^{2S+1}L_I$ now follows directly. The superscript is the spin multiplicity $2S+1$, the letter denotes $L = 0, 1, 2, \ldots \to S, P, D, \ldots$, and the subscript is the total angular momentum I. Hence the two even-parity possibilities are $^3S_1$ and $^3D_1$.

For later expectation values, the stretched states also fix the Clebsch–Gordan convention explicitly:

$$|^3S_1; 1, 1\rangle = |L{=}0, m_L{=}0\rangle |S{=}1, m_S{=}1\rangle, \tag{1.12}$$

$$|^3D_1; 1, 1\rangle = \sqrt{\frac{1}{10}}\,|2, 0\rangle|1, 1\rangle - \sqrt{\frac{3}{10}}\,|2, 1\rangle|1, 0\rangle + \sqrt{\frac{3}{5}}\,|2, 2\rangle|1, -1\rangle. \tag{1.13}$$

The squared coefficients sum to one. They give $\langle L_z \rangle = 3\hbar/2$ and $\langle S_z \rangle = -\hbar/2$, in agreement with the projection theorem below.

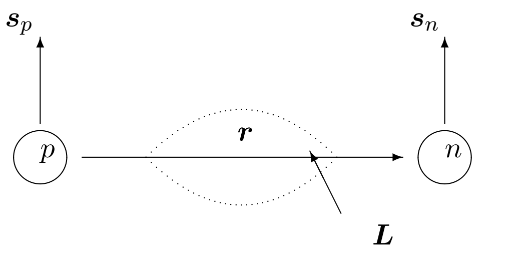

$$I^\pi = 1^+ : \; ^3S_1 \text{ dominant} + \text{small } ^3D_1$$

Figure 1.2: Schematic spins and orbital angular momentum in the NN system. The deuteron ground state is dominated by parallel spins and $L = 0$, with a small $L = 2$ admixture.

Key idea

Spin dependence of the nuclear force. Nature binds the triplet channel and not the singlet. The NN force depends on the relative orientation of the nucleon spins. A spin-independent central well would not explain that fact.

1.2.1 Triplet and singlet spin states

Start with the unique highest-projection product state,

$$|1,1\rangle = |\uparrow\uparrow\rangle. \tag{1.14}$$

Apply the total lowering operator $S_- = s_{p-} + s_{n-}$. Since $S_-|1,1\rangle = \hbar\sqrt{2}\,|1,0\rangle$,

$$S_-|\uparrow\uparrow\rangle = \hbar|\downarrow\uparrow\rangle + \hbar|\uparrow\downarrow\rangle, \tag{1.15}$$

$$\therefore \quad |1,0\rangle = \frac{1}{\sqrt{2}}\left(|\uparrow\downarrow\rangle + |\downarrow\uparrow\rangle\right). \tag{1.16}$$

A second lowering gives $|1,-1\rangle = |\downarrow\downarrow\rangle$. The three triplet states ($S = 1$) are therefore

$$|1,1\rangle = |\uparrow\uparrow\rangle, \qquad |1,0\rangle = \tfrac{1}{\sqrt{2}}(|\uparrow\downarrow\rangle + |\downarrow\uparrow\rangle), \qquad |1,-1\rangle = |\downarrow\downarrow\rangle. \tag{1.17}$$

The remaining normalized $M_S = 0$ combination must be orthogonal to $|1,0\rangle$; it is the singlet

$$|0,0\rangle = \tfrac{1}{\sqrt{2}}(|\uparrow\downarrow\rangle - |\downarrow\uparrow\rangle). \tag{1.18}$$

A useful operator that distinguishes them is $\boldsymbol{s}_p \cdot \boldsymbol{s}_n$. Square $\boldsymbol{S} = \boldsymbol{s}_p + \boldsymbol{s}_n$:

$$\boldsymbol{S}^2 = \boldsymbol{s}_p^2 + \boldsymbol{s}_n^2 + 2\boldsymbol{s}_p \cdot \boldsymbol{s}_n, \tag{1.19}$$

$$\therefore \quad \boldsymbol{s}_p \cdot \boldsymbol{s}_n = \frac{1}{2}\left(\boldsymbol{S}^2 - \boldsymbol{s}_p^2 - \boldsymbol{s}_n^2\right). \tag{1.20}$$

Because $s_p = s_n = \frac{1}{2}$, $\boldsymbol{s}_p^2 = \boldsymbol{s}_n^2 = \frac{3}{4}\hbar^2$. Thus

$$\langle \boldsymbol{s}_p \cdot \boldsymbol{s}_n \rangle = \frac{\hbar^2}{2}\left[S(S+1) - \frac{3}{4} - \frac{3}{4}\right] = \begin{cases} +\dfrac{\hbar^2}{4}, & S = 1, \\ -\dfrac{3\hbar^2}{4}, & S = 0. \end{cases} \tag{1.21}$$

A potential containing $\boldsymbol{\sigma}_p \cdot \boldsymbol{\sigma}_n$ can therefore deepen the triplet well relative to the singlet. That is why the square-well depth of Lecture 7 applies to the *triplet* channel; the singlet well is shallower and does not bind.

Caution

The singlet value is not zero. It is negative ($-3\hbar^2/4$). Saying the singlet product "vanishes" is a common slip; the correct eigenvalues matter when one writes $V_\sigma(r)$.

1.3 Magnetic moments: from classical orbits to g-factors

1.3.1 Nuclear magneton

Consider a charge e moving with speed v in a circular orbit of radius r. Its period, current, and loop area are

$$T = \frac{2\pi r}{v}, \qquad \mathcal{I} = \frac{e}{T} = \frac{ev}{2\pi r}, \qquad \mathcal{A} = \pi r^2. \tag{1.22}$$

The magnetic dipole moment is current times area,

$$\mu = \mathcal{I}\mathcal{A} = \frac{evr}{2}. \tag{1.23}$$

Since the orbital angular momentum is $L = mvr$, this becomes

$$\boldsymbol{\mu}_\ell = \frac{e}{2m}\boldsymbol{L}. \tag{1.24}$$

For a proton, set $m = m_p$ and factor out one quantum $\hbar$. This defines the **nuclear magneton**

$$\mu_N = \frac{e\hbar}{2m_p} \approx 3.15245 \times 10^{-8}\,\mathrm{eV/T}. \tag{1.25}$$

The displayed decimal is a rounded recommended-constant value; CODATA updates should be used when metrological precision matters. The lecture retains only the digits needed for the percent-level structure argument. It is smaller than the Bohr magneton by $m_e/m_p \approx 1/1836$. Ordinary magnetism of matter is electronic; nuclear magnetism is a delicate probe [6].

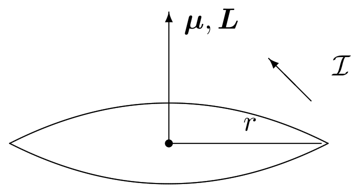

$$\mu = \mathcal{I}\pi r^2 = eL/(2m)$$

Figure 1.3: Classical orbital current: charge on a loop produces $\mu \propto qL/(2m)$. Neutrons have $q = 0$ and no orbital moment from net charge.

1.3.2 Orbital and spin contributions

We write

$$\mu_\ell = g_\ell\, \mu_N \frac{\ell_z}{\hbar}, \qquad \mu_s = g_s\, \mu_N \frac{s_z}{\hbar}. \tag{1.26}$$

For proton orbital motion $g_\ell = 1$; for the neutron $g_\ell = 0$. For free nucleon *spins*, measured magnetic moments, expressed in the CODATA-defined nuclear-magneton unit, give anomalous g-factors far from the Dirac value $g_s = 2$. Rounded for this calculation,

$$g_p = 5.5857, \tag{1.27}$$

$$g_n = -3.8261. \tag{1.28}$$

These are experimental nucleon properties, not predictions of CODATA; CODATA supplies the consistent constants and unit conversion. Equivalently, $\mu_p = +2.7928\,\mu_N$ and $\mu_n = -1.9130\,\mu_N$. The neutron's nonzero moment and the proton's large g_p are early evidence that nucleons are composite (meson clouds; today, quarks) [6, 2].

1.4 Deuteron magnetic moment: pure S-wave calculation

If the orbital angular momentum vanishes, there is no orbital magnetic moment: only the intrinsic spins of the proton and neutron contribute. With $I^\pi = 1^+$ and a pure $^3S_1$ configuration, the stretched state $M_I = 1$ has both spins aligned ($s_z = +\hbar/2$). The deuteron moment is then simply the sum of the free-nucleon moments [6],

$$\mu_d(L{=}0) = \mu_p + \mu_n = \frac{g_p + g_n}{2}\,\mu_N = \frac{5.5857 - 3.8261}{2}\,\mu_N = 0.8798\,\mu_N. \tag{1.29}$$

Experiment finds

$$\mu_d^{(\mathrm{exp})} = 0.8574376(4)\,\mu_N, \tag{1.30}$$

about $0.022\,\mu_N$ ($\sim 2.5\%$) below the pure S-wave value. The agreement is already striking: most of μ_d is indeed $\mu_p + \mu_n$. The residual deficit, however, is a genuine structural effect. Meson-exchange currents and relativistic corrections can shift the moment, but within the nonrelativistic NN picture the natural explanation is a small admixture of $L = 2$ in the ground-state wave function [6].

Key idea

Physics of the discrepancy. A pure s-wave deuteron would have $\mu_d = \mu_p + \mu_n$. The measured moment is slightly smaller, signalling a few-percent D-wave component and, with it, a non-central piece of the force.

1.5 D-wave admixture from μ_d

Write the ground state as a coherent mixture of even orbital waves allowed by $I^\pi = 1^+$,

$$|\psi\rangle = a_S\,|L{=}0\rangle + a_D\,|L{=}2\rangle, \qquad |a_S|^2 + |a_D|^2 = 1. \tag{1.31}$$

1.5.1 Expectation value of the magnetic-moment operator

The numerical D-state moment should not simply be quoted; it follows from an angular-momentum expectation value. In the centre-of-mass frame, and neglecting exchange currents, the z-component of the two-nucleon magnetic-moment operator is

$$\frac{\hat{\mu}_z}{\mu_N} = \frac{1}{2}\frac{\hat{L}_z}{\hbar} + g_p\frac{\hat{s}_{pz}}{\hbar} + g_n\frac{\hat{s}_{nz}}{\hbar}. \tag{1.32}$$

Only the proton contributes an orbital magnetic moment. Here $\boldsymbol{L} = \boldsymbol{r} \times \boldsymbol{p}$ always denotes the *relative* orbital angular momentum, not either particle's orbital momentum about an arbitrary laboratory origin. Its relation to the centre-of-mass orbital momenta can be obtained explicitly.

Let $M = m_p + m_n$, $\boldsymbol{r} = \boldsymbol{r}_p - \boldsymbol{r}_n$, and let $\boldsymbol{p}$ be the relative momentum in the centre-of-mass frame. Then

$$\boldsymbol{r}_p = \frac{m_n}{M}\boldsymbol{r}, \qquad \boldsymbol{p}_p = \boldsymbol{p}, \tag{1.33}$$

so

$$\boldsymbol{L}_p = \boldsymbol{r}_p \times \boldsymbol{p}_p = \frac{m_n}{M}\,\boldsymbol{r} \times \boldsymbol{p} = \frac{m_n}{M}\boldsymbol{L} \simeq \frac{1}{2}\boldsymbol{L}. \tag{1.34}$$

Similarly $\boldsymbol{L}_n = (m_p/M)\boldsymbol{L}$, but the neutron has zero one-body orbital charge factor. Thus the exact coefficient of L_z is m_n/M, approximated by 1/2 in Equation (1.32). This states the CM orbital convention completely. Within the spin-triplet state the proton and neutron share the total spin symmetrically. Equivalently, the antisymmetric operator $\boldsymbol{s}_p - \boldsymbol{s}_n$ has zero diagonal matrix element between symmetric triplet spin states, and therefore

$$\langle s_{pz}\rangle = \langle s_{nz}\rangle = \frac{1}{2}\langle S_z\rangle. \tag{1.35}$$

The projection theorem itself follows in two steps. First, $\boldsymbol{J} = \boldsymbol{L} + \boldsymbol{S}$ implies

$$\boldsymbol{L}\cdot\boldsymbol{J} = \boldsymbol{L}\cdot(\boldsymbol{L}+\boldsymbol{S}) = \boldsymbol{L}^2 + \boldsymbol{L}\cdot\boldsymbol{S}, \tag{1.36}$$

$$\boldsymbol{J}^2 = \boldsymbol{L}^2 + \boldsymbol{S}^2 + 2\boldsymbol{L}\cdot\boldsymbol{S}. \tag{1.37}$$

Eliminating $\boldsymbol{L}\cdot\boldsymbol{S}$ gives

$$\boldsymbol{L}\cdot\boldsymbol{J} = \frac{1}{2}\left(\boldsymbol{J}^2 + \boldsymbol{L}^2 - \boldsymbol{S}^2\right). \tag{1.38}$$

In a state $|LSJM\rangle$, rotational symmetry says that the expectation value of $\boldsymbol{L}$ can point only along $\boldsymbol{J}$. Its z-projection is consequently

$$\langle L_z\rangle = \frac{\langle \boldsymbol{L}\cdot\boldsymbol{J}\rangle}{J(J+1)\hbar^2}\,\langle J_z\rangle. \tag{1.39}$$

Using $\langle J_z\rangle = M\hbar$ and the eigenvalues of the squared angular momenta in Equation (1.38) gives

$$\langle L_z\rangle = M\hbar\,\frac{J(J+1)+L(L+1)-S(S+1)}{2J(J+1)}, \tag{1.40}$$

$$\langle S_z\rangle = M\hbar\,\frac{J(J+1)+S(S+1)-L(L+1)}{2J(J+1)}. \tag{1.41}$$

The second line can be obtained either by interchanging L and S or from $\langle S_z\rangle = M\hbar - \langle L_z\rangle$. The observable deuteron moment is evaluated in the stretched state $J = M = 1$.

For ${}^3S_1$, $L = 0$ and $S = 1$, so

$$\frac{\langle L_z\rangle}{\hbar} = 1\,\frac{1(1+1)+0(0+1)-1(1+1)}{2(1)(1+1)} = \frac{2+0-2}{4} = 0, \tag{1.42}$$

$$\frac{\langle S_z\rangle}{\hbar} = 1\,\frac{1(1+1)+1(1+1)-0(0+1)}{2(1)(1+1)} = \frac{2+2-0}{4} = 1. \tag{1.43}$$

Equation (1.32) therefore reproduces

$$\begin{aligned}\mu(^3S_1) &= \left[\frac{1}{2}(0) + \frac{g_p + g_n}{2}(1)\right]\mu_N \\ &= \frac{g_p + g_n}{2}\,\mu_N = \mu_p + \mu_n = 0.8798\,\mu_N. \end{aligned} \tag{1.44}$$

For $^3D_1$, $L = 2$, $S = 1$, and $J = M = 1$. Equations (1.40)–(1.41) give, step by step,

$$\frac{\langle L_z\rangle}{\hbar} = 1\,\frac{1(1+1) + 2(2+1) - 1(1+1)}{2(1)(1+1)} = \frac{2+6-2}{4} = \frac{3}{2}, \tag{1.45}$$

$$\frac{\langle S_z\rangle}{\hbar} = 1\,\frac{1(1+1) + 1(1+1) - 2(2+1)}{2(1)(1+1)} = \frac{2+2-6}{4} = -\frac{1}{2}. \tag{1.46}$$

The orbital and spin angular momenta are therefore partly antiparallel in the D state. Substitution into (1.32) yields

$$\begin{aligned}\mu(^3D_1) &= \left[\frac{1}{2}\left(\frac{3}{2}\right) + \frac{g_p + g_n}{2}\left(-\frac{1}{2}\right)\right]\mu_N \\ &= \frac{1}{4}(3 - g_p - g_n)\,\mu_N \approx 0.310\,\mu_N. \end{aligned} \tag{1.47}$$

This is the expectation-value derivation of the smaller pure-D magnetic moment [6, 2].

In the one-body operator approximation, $\langle ^3S_1|\hat{\mu}_z|^3D_1\rangle = 0$: the angular functions with $L = 0$ and $L = 2$ are orthogonal, and the operator in (1.32) does not change L. The mixed-state expectation value can be expanded before the cross terms are discarded:

$$\begin{aligned}\langle\psi|\hat{\mu}_z|\psi\rangle &= |a_S|^2\langle ^3S_1|\hat{\mu}_z|^3S_1\rangle + |a_D|^2\langle ^3D_1|\hat{\mu}_z|^3D_1\rangle \\ &\quad + a_S^* a_D\langle ^3S_1|\hat{\mu}_z|^3D_1\rangle + a_D^* a_S\langle ^3D_1|\hat{\mu}_z|^3S_1\rangle \\ &= P_S\mu_S + P_D\mu_D. \end{aligned} \tag{1.48}$$

Therefore

$$\mu_d = P_S\,(0.880\,\mu_N) + P_D\,(0.310\,\mu_N), \qquad P_S + P_D = 1. \tag{1.49}$$

To obtain the commonly used form, substitute $P_S = 1 - P_D$ and $\mu_D = \frac{1}{4}(3 - g_p - g_n)\mu_N$:

$$\begin{aligned}\mu_d &= (1 - P_D)(\mu_p + \mu_n) + P_D\frac{3 - g_p - g_n}{4}\mu_N \\ &= (\mu_p + \mu_n) + P_D\left[\frac{3}{4}\mu_N - \frac{3}{2}(\mu_p + \mu_n)\right] \\ &= (\mu_p + \mu_n) - \frac{3}{2}\left[\mu_p + \mu_n - \frac{1}{2}\mu_N\right]P_D. \end{aligned} \tag{1.50}$$

Finally, requiring $\mu_d = 0.8574\,\mu_N$ and retaining the displayed rounded moments gives

$$\begin{aligned} 0.8574 &= 0.8798(1-P_D) + 0.310P_D \\ &= 0.8798 - (0.8798-0.310)P_D, \end{aligned} \tag{1.51}$$

$$\begin{aligned} (0.8798-0.310)P_D &= 0.8798 - 0.8574, \\ P_D &= \frac{0.8798-0.8574}{0.8798-0.310} = 0.0393 \approx 0.039, \qquad P_S = 1 - P_D \approx 0.961. \end{aligned} \tag{1.52}$$

This classroom estimate suggests a few-percent D-wave. It is *not* a model-independent measurement of P_D: meson-exchange currents and relativistic corrections also shift μ_d. Independent NN scattering analyses still find a few-percent D-state probability, so the qualitative conclusion is robust: the force cannot be purely central. Only a tensor interaction can mix $L = 0$ with $L = 2$ in a single eigenstate. The electric quadrupole moment $Q_d \neq 0$ (Lecture 9) establishes that mixing far more cleanly than the magnetic-moment deficit alone [6].

Caution

Do not promote $P_D \approx 4\%$ to an observable. Treat it as a pedagogical estimate that motivates looking for a tensor force; the decisive geometric evidence is the nonzero quadrupole moment.

Key idea

What Lectures 7–9 establish together. Weak binding fixes the depth and range of the residual force. Spin and parity fix the channel as mostly ${}^3S_1$. The magnetic-moment deficit *suggests* a small D-wave; the quadrupole moment *requires* one, and with it a tensor force.

1.6 Preview of heavier nuclei

In odd-A nuclei, pairing often cancels the moments of all but the last unpaired nucleon. Plotting μ versus I produces the Schmidt lines. Real nuclei fall between those lines because of configuration mixing, the many-body cousin of the deuteron's D-wave. The deuteron is the cleanest few-body example of the same idea: free moments first, then a small admixture [6, 1].

Takeaway

Takeaways (Lecture 8).

- $I^\pi = 1^+$: even parity forces even L; the bound state is spin triplet.
- Spin-dependent force: triplet binds, singlet does not.
- Pure S-wave $\mu_d = 0.880\,\mu_N$; experiment $0.857\,\mu_N$.
- Mixture $\sim 96\%\ S + \sim 4\%\ D$ is a classroom estimate of the magnetic deficit; quadrupole data (next lecture) establish the D-wave and the tensor force.

1.7 Deeper physics: magnetic moments beyond the deuteron

1.7.1 How μ is measured (Rabi and NMR)

Place a state of angular momentum I in a uniform field $\boldsymbol{B} = B\hat{\boldsymbol{z}}$. With $\hat{\mu}_z = g_I \mu_N \hat{I}_z/\hbar$, the Zeeman Hamiltonian is

$$\hat{H}_Z = -\hat{\boldsymbol{\mu}} \cdot \boldsymbol{B} = -g_I \mu_N B \frac{\hat{I}_z}{\hbar}. \tag{1.53}$$

Because $\hat{I}_z|I, M_I\rangle = M_I \hbar |I, M_I\rangle$,

$$E_{M_I} = -g_I \mu_N B M_I. \tag{1.54}$$

Adjacent substates therefore differ by

$$|\Delta E| = g_I \mu_N B = h\nu. \tag{1.55}$$

The Rabi molecular-beam method and nuclear magnetic resonance detect the frequency ν at which a radiofrequency field drives $\Delta M_I = \pm 1$ transitions. Since B is known, the resonance gives g_I, and the stretched-state moment is $\mu = g_I I \mu_N$. Free-nucleon moments $\mu_p = +2.7928\,\mu_N$ and $\mu_n = -1.9130\,\mu_N$ are among the most accurately known quantities in nuclear physics [2, 1].

1.7.2 Schmidt lines (preview of the shell model)

For odd-A nuclei the magnetic moment is often dominated by the last unpaired nucleon. Plotting μ versus I produces the Schmidt lines: two limiting curves for $j = \ell \pm \frac{1}{2}$. Real nuclei fall between the lines because of configuration mixing and meson-exchange currents. The deuteron is the few-body cousin of that story: free $\mu_p + \mu_n$ is the extreme independent-particle limit; a few-percent D-wave admixture is the simplest configuration mixing [6, 1]. The two Schmidt formulae are derived, rather than merely quoted, in Section 1.9.2.

1.7.3 Isospin language

Proton and neutron form an isospin doublet $t = \frac{1}{2}$. The deuteron has total isospin $T = 0$, and this assignment follows from exchange symmetry. For two nucleons, the spatial, spin, and isospin factors acquire under exchange the signs

$$(-1)^L, \qquad (-1)^{S+1}, \qquad (-1)^{T+1}, \tag{1.56}$$

respectively. Their product must be -1 for fermions, so

$$(-1)^{L+S+T} = -1. \tag{1.57}$$

The deuteron has even L and $S = 1$. Hence $L + S + T$ is odd only when $T = 0$. Explicitly, its isospin wave function is the antisymmetric combination

$$|T = 0, T_z = 0\rangle = \frac{1}{\sqrt{2}} \left(|pn\rangle - |np\rangle \right). \tag{1.58}$$

The $T = 1$, $S = 0$ pn partner of the virtual ${}^1S_0$ state is unbound, as are free nn and pp (after Coulomb). Charge independence of the strong force organises NN scattering lengths into a nearly universal pattern once Coulomb is removed. Lecture 10 develops this NN spin–isospin structure through phase shifts [4].

Remark

Quarks and anomalous moments. Dirac particles with charge e and mass m have $g = 2$. The proton's $g_p \approx 5.59$ and the neutron's nonzero moment are direct evidence of composite structure (charged quark currents and meson clouds), already anticipated in Lecture 7's residual-force discussion [2, 4].

1.7.4 Beyond the one-body magnetic operator

For the one-body operator derived in Section 1.5.1, the S–D cross term vanishes: $\hat{L}_z$, $\hat{s}_{pz}$, and $\hat{s}_{nz}$ do not change L, and the $L = 0$ and $L = 2$ angular functions are orthogonal. This gives the probability-weighted expectation value in Equation (1.50).

A precision calculation must add two-body meson-exchange currents, relativistic corrections, and small nucleon-structure effects. Those contributions alter the magnetic moment without being equivalent to a change in P_D. Modern potentials still find a few-percent D-state probability, so the classroom estimate is useful, but P_D itself is model dependent [6].

1.8 Magnetic moment deficit and D-wave probability

1.8.1 From free sum to measured μ_d

The independent-particle estimate $\mu_S \approx \mu_p + \mu_n = 0.8798\,\mu_N$ overshoots experiment ($\mu_d = 0.8574\,\mu_N$) by about 2.5%. The lecture attributes the deficit to a small ${}^3D_1$ admixture: orbital motion of the proton in $L = 2$ contributes $g_\ell^{(p)}\mu_N\langle L_z\rangle$, while the S–D interference shifts the spin projections. Keeping only the dominant S-wave spin term plus a D-wave orbital correction with probability P_D gives the schematic balance

$$\mu_d \approx (1 - P_D)(\mu_p + \mu_n) + P_D\, g_\ell^{(p)}\, \langle L_z\rangle_D, \tag{1.59}$$

where $\langle L_z\rangle_D$ is fixed by angular-momentum algebra in the stretched state $M_I = 1$.

1.8.2 A worked P_D estimate

Using $g_\ell^{(p)} = 1$ and typical shell-model couplings for $L = 2$, $S = 1$, $J = 1$, a few-percent D-wave probability suffices:

$$P_D \sim \frac{\mu_p + \mu_n - \mu_d}{(\mu_p + \mu_n) - g_\ell^{(p)}\langle L_z\rangle_D} \approx 0.04\text{–}0.06. \tag{1.60}$$

Inserting $P_D = 0.05$ into (1.59) lowers μ_d by $\sim 0.02\,\mu_N$, matching the observed deficit. The same P_D feeds the quadrupole moment (Lecture 9): μ_d and Q_d are correlated constraints on the tensor force, not independent knobs.

Key idea

Schmidt preview. Odd-A nuclei use the same logic at higher A: plot μ/μ_N versus I and compare with the Schmidt lines for $j = \ell \pm \frac{1}{2}$ (Section 1.9.2). The deuteron is the two-body limit where only one pair of nucleons contributes and configuration mixing is a few-percent D-wave rather than valence-shell fragmentation.

Remark

What P_D is not. Meson-exchange currents and relativistic corrections also shift μ_d at the percent level. Treating the entire deficit as orbital D-wave probability is a classroom estimate, not a unique inversion of data. Modern potentials quote P_D with model-dependent spread; the qualitative lesson (tensor force required) is robust [6, 2].

1.8.3 Isospin and the magnetic moment sum rule

In the $T = 0$ deuteron, the isospin wave function is antisymmetric under nucleon exchange (Section 1.7.3). The magnetic operator is isovector, so the $T = 0$ expectation value is not constrained to equal $\mu_p + \mu_n$ unless the spatial wave function is purely S-wave. The measured $\mu_d < \mu_p + \mu_n$ is therefore a joint statement about isospin symmetry and tensor-induced D-wave admixture. For comparison, the unbound $T = 1$, $S = 0$ virtual state has no stable magnetic moment, but its scattering length $a_s \approx -23.7\,\text{fm}$ (Lecture 10) shows how close the singlet channel comes to binding despite $\mu_p + \mu_n$ being irrelevant there.

1.8.4 Schmidt lines at $A = 2$ and $A = 15$

At $A = 2$ the "valence nucleon" picture is replaced by two active bodies, yet the logic survives: start from free moments, then reduce by orbital mixing. At $A = 15$, ^{15}N ($I = \frac{1}{2}^-$) and ^{15}O ($I = \frac{1}{2}^-$) provide mirror tests of Schmidt limits once the hole/particle sign is tracked. Lecture 14 plots the full Schmidt curves; the deuteron is the anchor point showing that even the simplest bound nucleus requires configuration mixing beyond free g-factors [1, 22].

Impulse versus consistent currents

State in one sentence the impulse approximation for μ_d and in a second sentence what "consistent two-body currents" means. That pair of sentences is the conceptual payload of Lecture 8 beyond the existence of a D-wave.

1.9 Further physics: magnetic moments and the nuclear magneton

To each angular momentum is associated a magnetic dipole

$$\boldsymbol{\mu} = g\,\mu_N \frac{\boldsymbol{j}}{\hbar}, \qquad \mu_N = \frac{e\hbar}{2m_p}. \tag{1.61}$$

For orbital motion of a proton, $g_\ell = 1$; for a neutron, $g_\ell = 0$. Spin g-factors of free nucleons are anomalous ($g_p \approx 5.59$, $g_n \approx -3.83$), a signal of internal structure [13, 6, 2, 5].

In odd-A nuclei a first approximation attributes μ to the last unpaired nucleon (Schmidt estimate). The deuteron is the clean two-body limit of the same idea: free moments first, then a small configuration admixture (D-wave) to match experiment. Exact g-factors of complex nuclei require interactions among many nucleons; the deuteron isolates the few-body physics.

1.9.1 Spin dependence from the deuteron alone

From $I^\pi = 1^+$ and $\mu_d \approx \mu_p + \mu_n$ one concludes that the ground state is mostly ${}^3S_1$. The absence of a bound ${}^1S_0$ pn state shows that the force is spin-dependent: both channels are attractive, but only the triplet is deep enough to bind [14, 6]. The small quadrupole moment and the μ_d deficit then require a few-percent ${}^3D_1$ admixture (tensor force; Lecture 9).

1.9.2 Schmidt lines for odd-A nuclei

For a single valence nucleon with orbital angular momentum ℓ and spin $s = \frac{1}{2}$, the one-body magnetic operator is

$$\frac{\hat{\mu}_z}{\mu_N} = g_\ell \frac{\hat{\ell}_z}{\hbar} + g_s \frac{\hat{s}_z}{\hbar}. \tag{1.62}$$

The measured moment is the expectation value in the stretched state $|j, m = j\rangle$. Since $j_z = \ell_z + s_z$, it is useful to write

$$\frac{\mu}{\mu_N} = g_\ell j + (g_s - g_\ell)\frac{\langle s_z\rangle}{\hbar}. \tag{1.63}$$

The projection theorem derived in Section 1.5.1, with $L \to \ell$, $S \to s$, and $M = j$, gives

$$\frac{\langle s_z\rangle}{\hbar} = j\,\frac{j(j+1) + s(s+1) - \ell(\ell+1)}{2j(j+1)}. \tag{1.64}$$

For aligned spin, $j = \ell + \frac{1}{2}$, so $\ell = j - \frac{1}{2}$ and $s(s+1) = \frac{3}{4}$. Substitution into Equation (1.64) gives

$$\begin{aligned}\frac{\langle s_z\rangle}{\hbar} &= \frac{j(j+1) + \frac{3}{4} - (j-\frac{1}{2})(j+\frac{1}{2})}{2(j+1)} \\ &= \frac{j^2 + j + \frac{3}{4} - (j^2 - \frac{1}{4})}{2(j+1)} = \frac{j+1}{2(j+1)} = \frac{1}{2}.\end{aligned} \tag{1.65}$$

Equation (1.63) then yields the upper Schmidt line,

$$\boxed{\frac{\mu}{\mu_N} = g_\ell j + \frac{1}{2}(g_s - g_\ell), \qquad j = \ell + \frac{1}{2}.} \tag{1.66}$$

Equivalently, $\mu/\mu_N = g_\ell \ell + g_s/2$: in the stretched state the orbital and spin projections are simply ℓ and $1/2$.

For anti-aligned spin, $j = \ell - \frac{1}{2}$, so $\ell = j + \frac{1}{2}$. Now

$$\begin{aligned}\frac{\langle s_z \rangle}{\hbar} &= \frac{j(j+1) + \frac{3}{4} - (j+\frac{1}{2})(j+\frac{3}{2})}{2(j+1)} \\ &= \frac{j^2 + j + \frac{3}{4} - (j^2 + 2j + \frac{3}{4})}{2(j+1)} = -\frac{j}{2(j+1)}.\end{aligned} \tag{1.67}$$

The lower Schmidt line is therefore

$$\boxed{\frac{\mu}{\mu_N} = g_\ell j - (g_s - g_\ell)\frac{j}{2(j+1)}, \qquad j = \ell - \frac{1}{2}.} \tag{1.68}$$

For an unpaired proton one inserts $g_\ell = 1$ and $g_s = g_p$; for an unpaired neutron, $g_\ell = 0$ and $g_s = g_n$. These are independent particle limits, not exact predictions. Experimental moments of odd-A nuclei generally lie between the Schmidt lines, shifted toward smaller $|\mu|$ by configuration mixing and meson-exchange currents [6, 2, 13]. The deuteron is the few-body prototype of that programme: start from free g-factors, then correct for orbital admixtures.

1.9.3 Nuclear magneton vs Bohr magneton

Because $m_p \approx 1836\, m_e$,

$$\begin{aligned}\mu_N &= \frac{m_e}{m_p}\,\mu_B \\ &= \frac{m_e}{m_p}\left(\frac{e\hbar}{2m_e}\right) = \frac{e\hbar}{2m_p} \\ &\approx \frac{1}{1836}\,\mu_B.\end{aligned} \tag{1.69}$$

Nuclear moments are therefore three orders of magnitude smaller than electronic moments, which is why nuclear magnetism is a precision hyperfine effect in atoms and a separate experimental industry (NMR, atomic beams, ion traps) [5, 2].

1.9.4 Projection theorem for $\langle s_z \rangle$

The Schmidt derivation (Section 1.9.2) rests on evaluating $\langle s_z \rangle$ in $|j, m = j\rangle$. For coupled $\boldsymbol{L} + \boldsymbol{S} = \boldsymbol{J}$, the Wigner–Eckart theorem gives

$$\frac{\langle s_z \rangle}{\hbar} = \frac{\langle \boldsymbol{J} \cdot \boldsymbol{S} \rangle}{j(j+1)\hbar^2}\, j = j\,\frac{j(j+1) + s(s+1) - \ell(\ell+1)}{2j(j+1)}, \tag{1.70}$$

which is (1.64). For the deuteron ($\ell \to L = 0$, $s \to S = 1$, $j \to I = 1$), $\langle S_z \rangle/\hbar = 0$ in the pure S-wave limit, so $\mu_S = \mu_p + \mu_n$ follows immediately. Only $L = 2$ admixture generates nonzero $\langle L_z \rangle$ and S–D cross terms in the full operator of Section 1.5.1.

1.9.5 Worked Schmidt comparison for ^{15}N

^{15}N ($Z = 7$, one proton hole on ^{16}O) has $I = \frac{1}{2}$ from the $1p_{1/2}$ orbit ($\ell = 1$, $j = \frac{1}{2}$). The lower Schmidt line with $g_\ell = 1$, $g_s = g_p$ gives

$$\frac{\mu}{\mu_N} = \frac{1}{2} + \frac{1}{2}(g_p - 1)\frac{1/2}{3/2} = \frac{1}{2} + \frac{1}{6}(g_p - 1) \approx 0.44, \tag{1.71}$$

so $\mu_{\text{Schmidt}} \approx 2.2\,\mu_N$. Experiment gives $\mu = -0.283\,\mu_N$: the hole sign and core polarisation reverse and reduce the moment, showing that Schmidt lines are bounds, not predictions, even near closed shells [6, 22]. The deuteron sits closer to the independent-particle limit because only two nucleons participate.

1.9.6 Link to Lecture 9 and 14

The same D-wave probability that lowers μ_d generates Q_d (Lecture 9) through (**??**). Lecture 14 generalises the Schmidt plot to all odd-A nuclei and introduces quenching of g_s. The deuteron is the minimal laboratory for all three ideas: anomalous free-nucleon g-factors, configuration mixing, and tensor-force induced orbital admixture [2].

1.9.7 Rabi resonance in the lab frame

In NMR one typically applies a transverse radiofrequency field $B_1 \cos\omega t$ near the Larmor frequency $\omega_0 = g\mu_N B/\hbar$. The Rabi condition $\hbar\omega = g\mu_N B$ is the same physics as the molecular-beam $\Delta M = \pm 1$ resonance, but in a condensed sample the signal is detected as a voltage induced in a pickup coil. For the deuteron, the small D-wave correction shifts ω_0 by parts per thousand relative to $\mu_p + \mu_n$, comparable to the shift used to infer P_D in precision beam experiments [2, 22].

1.9.8 Hyperfine structure in atomic deuterium

Replacing the proton in hydrogen by a deuteron changes the hyperfine splitting because $\mu_d \neq \mu_p$. The $1S$ hyperfine interval scales as $\mu_d I_d \cdot \langle \boldsymbol{I} \cdot \boldsymbol{J} \rangle$ for the electron coupling. The percent-level difference between μ_d and $\mu_p + \mu_n$ is therefore visible in atomic spectroscopy, independent of nuclear scattering experiments. Atomic and molecular data provide a third route to the same D-wave physics constrained by μ_d and Q_d (Lecture 9) [2, 6].

1.10 Deeper reading: μ_d, exchange currents, and Schmidt intuition

The deuteron magnetic moment lies close to but not exactly at $\mu_p + \mu_n$. A small D-wave admixture P_D shifts μ_d by an amount proportional to $(\mu_p + \mu_n - \frac{1}{2}\mu_N)$. Fitting μ_d alone does not fix P_D uniquely once meson-exchange currents are allowed: two-body currents can move μ_d at the same order as a change in P_D. Modern calculations therefore evaluate the current operator consistently with the Hamiltonian that generates the wave function.

Order of magnitude

If a pure S-wave estimate gives $\mu_S \approx 0.880\,\mu_N$ and the measured $\mu_d \approx 0.857\,\mu_N$, a few-percent P_D accounts for the difference in the impulse approximation. Exchange currents of relative size $\sim 1\%$ matter at the same level: that is why Lecture 8's message is qualitative structure ($I^\pi = 1^+$ requires D-wave) rather than a precision extraction of P_D from μ_d alone.

Schmidt lines in Lecture 14 reuse the same single-particle magnetic operators; quenching and two-body currents reappear there in heavier nuclei. The deuteron is the cleanest few-body laboratory in which those operator issues can be stated without a large valence space.

Relativistic and two-body current bookkeeping

Relativistic corrections to magnetic operators and explicit meson-exchange currents enter at similar numerical size for μ_d. Calculations that vary one while freezing the other can appear to "prefer" a particular P_D. The reliable approach is a single Hamiltonian with consistent currents. That standard, learned on the deuteron, reappears in medium-mass Gamow–Teller quenching (Lectures 14 and 19).

Spin and isospin structure

The deuteron is isoscalar ($T = 0$). Its magnetic moment therefore tests isoscalar combinations of nucleon moments and isoscalar exchange currents. Isovector magnetic properties appear more strongly in odd-mirror pairs and in $N = Z$ odd–odd nuclei. Keeping isoscalar versus isovector channels straight prevents mis-applying deuteron lessons to Schmidt deviations in heavy nuclei.

From μ_d to many-body operators

Write $\mu_d = \mu_S(1 - P_D) + \mu_D P_D$ with the textbook combinations of nucleon moments. Insert $P_D = 0.04$ and 0.06 and compare with experiment. The residual can be assigned either to a adjusted P_D or to an exchange-current shift of a few hundredths of a nuclear magneton. Without an independent constraint (quadrupole moment, form factors, or a consistent current calculation), that assignment is ambiguous.

This ambiguity is the few-body prototype of operator renormalisation in heavy nuclei. Lecture 14's Schmidt deviations and Lecture 19's Gamow–Teller quenching are the same story at larger mass: wave functions and operators must be improved together. Keep a short notebook table: observable, impulse-approximation prediction, size of two-body current correction, and whether the correction is isoscalar or isovector. The deuteron fills the first row of that table.

Magnetic moments diagnose operators. The deuteron teaches the lesson in a system small enough to solve; medium-mass nuclei reuse it under the names quenching and effective g-factors.

In practice, rework one numerical estimate from the lecture with a different parameter set and compare the shift to the quoted experimental uncertainty. If the shift exceeds the uncertainty, the estimate is teaching a scale, not delivering a fit. That distinction keeps theoretical cartoons honest when they sit beside evaluated data tables and modern many-body calculations. Along the course arc, write one sentence linking this chapter backward and one forward: the discipline of those two sentences is as important as any single formula. Examination problems rarely ask for a literature review, but they do ask for the scale argument that literature reviews presuppose.

Research frontier: currents, D-wave, and student projects

Lecture 8 showed that the deuteron magnetic moment μ_d and the assignment $I^\pi = 1^+$ require a few-percent D-wave admixture in the ground state. Contemporary calculations evaluate two-body meson-exchange currents and relativistic corrections consistently with the same chiral Hamiltonian used for the wave function, rather than adding ad hoc current operators after the fact [41]. Related electroweak currents underlie Gamow–Teller quenching and neutrinoless double-beta matrix elements in heavier nuclei: a landmark ab initio study showed that consistent two-body currents resolve much of the long-standing GT quenching puzzle [50]. Precision tables of magnetic moments remain essential benchmarks for both few-body and shell-model calculations [22]. What remains uncertain is how large residual quenching is in mid-mass and heavy nuclei once two-body currents and correlations are both included, and how those lessons translate into $0\nu\beta\beta$ operator uncertainties.

Polarisation observables and electromagnetic form factors of the deuteron provide additional constraints on the same D-wave physics. Modern analyses insist that the current operator and the wave function come from one consistent framework; otherwise apparent agreement with μ_d can hide cancelling mistakes. That consistency requirement is the bridge from the lecture toy model to contemporary few-body papers.

Those consistency checks also matter for polarisation transfer and for deuteron electrodisintegration, where different current recipes can shift extracted P_D values.

Student directions. (1) Analytic estimate: recompute μ_S and μ_D contributions for a given P_D. (2) Data project: using Stone's table, plot odd-proton Schmidt deviations for $20 \le Z \le 40$. (3) Short essay: explain why exchange currents matter more for magnetic moments than for the charge radius.

1.11 Problems with solutions

Problem 8.1 — Pure S-wave magnetic moment

Using $g_p = 5.5857$ and $g_n = -3.8261$, compute the pure $^3S_1$ prediction for μ_d and the fractional difference from the experimental value $0.8574\,\mu_N$.

Solution 8.1

$$\mu_d(L{=}0) = \frac{g_p + g_n}{2}\,\mu_N = \frac{5.5857 - 3.8261}{2}\,\mu_N = 0.8798\,\mu_N.$$

$$\Delta\mu = 0.8798 - 0.8574 = 0.0224\,\mu_N, \qquad \frac{\Delta\mu}{\mu_d(L{=}0)} \approx 2.5\%.$$

Most of μ_d is $\mu_p + \mu_n$; the small deficit is structural [6].

Problem 8.2 — D-wave probability from μ_d

Assume

$$\mu_d = P_S\,(0.8798\,\mu_N) + P_D\,(0.310\,\mu_N), \quad P_S + P_D = 1,$$

and $\mu_d = 0.8574\,\mu_N$. Find P_D.

Solution 8.2

$$0.8574 = 0.8798(1 - P_D) + 0.310\,P_D = 0.8798 - 0.5698\,P_D,$$

$$P_D = \frac{0.8798 - 0.8574}{0.5698} \approx 0.039 \approx 4\%, \quad P_S \approx 96\%.$$

This 4% is a one-body-operator, model-dependent classroom inference, not an observable: exchange currents, relativistic corrections, and the chosen NN potential shift the extracted P_D. The robust conclusion is only that a few-percent D-wave is natural [6, 14].

Problem 8.3 — Why $L = 1$ is excluded

List (S, L) combinations that can give $I = 1$ for pn and show which survive the experimental parity $\pi = +$.

Solution 8.3

Coupling the two spin-$\frac{1}{2}$ nucleons first gives

$$S = \left|\tfrac{1}{2} - \tfrac{1}{2}\right|, \ldots, \tfrac{1}{2} + \tfrac{1}{2} = 0,\ 1.$$

Angular-momentum addition then requires

$$|L - S| \le I \le L + S.$$

For $S = 0$, this reduces to $I = L$, so $I = 1$ requires $L = 1$. For $S = 1$, requiring $I = 1$ gives

$$|L - 1| \le 1 \le L + 1,$$

which is satisfied by $L = 0, 1, 2$. Thus the four possibilities are

$$(S, L) = (0, 1),\ (1, 0),\ (1, 1),\ (1, 2).$$

Parity is $\pi = (-1)^L$. The measured $\pi = +$ eliminates both $L = 1$ cases, leaving $(S, L) = (1, 0)$ and $(1, 2)$, or ${}^3S_1$ and ${}^3D_1$. Both have $S = 1$, so the bound state is entirely spin triplet even though it is not entirely S-wave [6].

Problem 8.4 — Nuclear magneton scale

Compute $\mu_N = e\hbar/(2m_p)$ in MeV/T using $e\hbar/(2m_e) = \mu_B = 5.788 \times 10^{-11}$ MeV/T and $m_p/m_e = 1836$. Why is nuclear magnetism hard to measure compared with electronic magnetism?

Solution 8.4

$$\mu_N = \frac{m_e}{m_p}\,\mu_B = \frac{5.788 \times 10^{-11}}{1836} \approx 3.15 \times 10^{-14}\,\text{MeV/T}.$$

Nuclear moments are ~ 2000 times smaller than electronic ones, so they appear only as tiny hyperfine shifts or require specialised methods (Rabi beams, NMR) [5, 2].

Problem 8.5 — Derive the $^3D_1$ magnetic moment

For a pure $^3D_1$ state, use the projection theorem to calculate $\langle L_z\rangle$ and $\langle S_z\rangle$ in the stretched state $J = M = 1$. Then evaluate

$$\frac{\hat{\mu}_z}{\mu_N} = \frac{1}{2}\frac{\hat{L}_z}{\hbar} + \frac{g_p + g_n}{2}\frac{\hat{S}_z}{\hbar}$$

and obtain the numerical moment using the g-factors of Problem 8.1.

Solution 8.5

For $L = 2$, $S = 1$, and $J = M = 1$,

$$\begin{aligned}
\frac{\langle L_z\rangle}{\hbar} &= M\,\frac{J(J+1) + L(L+1) - S(S+1)}{2J(J+1)} \\
&= \frac{2+6-2}{4} = \frac{3}{2}, \\
\frac{\langle S_z\rangle}{\hbar} &= M\,\frac{J(J+1) + S(S+1) - L(L+1)}{2J(J+1)} \\
&= \frac{2+2-6}{4} = -\frac{1}{2}.
\end{aligned}$$

The magnetic moment is therefore

$$\begin{aligned}
\frac{\mu(^3D_1)}{\mu_N} &= \frac{1}{2}\left(\frac{3}{2}\right) + \frac{g_p+g_n}{2}\left(-\frac{1}{2}\right) \\
&= \frac{3}{4} - \frac{g_p+g_n}{4} = \frac{1}{4}(3 - g_p - g_n).
\end{aligned}$$

Numerically,

$$\begin{aligned}
3 - g_p - g_n &= 3 - 5.5857 - (-3.8261) \\
&= 3 - 5.5857 + 3.8261 = 1.2404, \\
\therefore \qquad \mu(^3D_1) &= \frac{1.2404}{4}\,\mu_N = 0.3101\,\mu_N.
\end{aligned}$$

[6].

Problem 8.6 — Charge independence and no bound nn

Explain why charge independence of the strong force, together with the Pauli principle, is consistent with a bound pn ($s = 1$) deuteron and no bound nn or pp systems.

Solution 8.6

For two nucleons the exchange sign is

$$(-1)^L(-1)^{S+1}(-1)^{T+1} = (-1)^{L+S+T},$$

and Fermi statistics require this sign to be -1. In an S-wave, $L = 0$, so $S + T$ must be odd. The deuteron channel has $S = 1$, hence $T = 0$. Its isospin state

$$\frac{1}{\sqrt{2}}(|pn\rangle - |np\rangle)$$

has no nn or pp member: two identical nucleons necessarily have $T = 1$. For nn or pp with $L = 0$ and $T = 1$, antisymmetry therefore forces $S = 0$. Charge independence relates that channel to the unbound $T = 1$, ${}^1S_0$ pn channel, apart from electromagnetic and small charge-dependent effects. Thus the bound $T = 0$, ${}^3S_1$ channel exists only for pn, while the allowed nn and pp S-wave channel does not bind [14, 6].

Problem 8.7 — Clebsch–Gordan check of the D state

Using Equation (1.13), verify normalisation and calculate $\langle L_z\rangle$ and $\langle S_z\rangle$ directly from the three product-state probabilities.

Solution 8.7

The probabilities are $1/10$, $3/10$, and $3/5$, whose sum is one. Therefore

$$\frac{\langle L_z\rangle}{\hbar} = \frac{1}{10}(0) + \frac{3}{10}(1) + \frac{3}{5}(2) = \frac{3}{2},$$

and

$$\frac{\langle S_z\rangle}{\hbar} = \frac{1}{10}(1) + \frac{3}{10}(0) + \frac{3}{5}(-1) = -\frac{1}{2}.$$

Their sum is $M = 1$, as required.

Bibliography

[1] R. A. Dunlap, *An Introduction to the Physics of Nuclei and Particles* (2nd ed.), IOP Publishing, Bristol (2023), DOI: 10.1088/978-0-7503-6094-4, Ch. 3 (Nuclear composition and size).

[2] W. Demtröder, *Nuclear and Particle Physics*, Undergraduate Lecture Notes in Physics, Springer, Cham (2023).

[3] S. Petrera, *Problems and Solutions in Nuclear and Particle Physics*, UNITEXT for Physics, Springer, Cham (2019).

[4] F. Terranova, *A Modern Primer in Particle and Nuclear Physics*, Oxford University Press (2021).

[5] S. D'Auria, *Introduction to Nuclear and Particle Physics*, Undergraduate Lecture Notes in Physics, Springer, Cham (2018).

[6] K. S. Krane, *Introductory Nuclear Physics*, Wiley, New York (1988).

[7] R. Hofstadter, "Electron scattering and nuclear structure," Rev. Mod. Phys. **28**, 214 (1956).

[8] H. F. Ehrenberg, R. Hofstadter, U. Meyer-Berkhout, D. G. Ravenhall, and S. E. Sobottka, "High-Energy Electron Scattering and the Charge Distribution of Carbon-12 and Oxygen-16," Phys. Rev. **113**, 666 (1959).

[9] H. Yukawa, "On the interaction of elementary particles. I," Proc. Phys.-Math. Soc. Japan **17**, 48 (1935).

[10] R. D. Woods and D. S. Saxon, "Diffuse surface optical model for nucleon-nuclei scattering," Phys. Rev. **95**, 577 (1954).

[11] H. G. J. Moseley, "The high-frequency spectra of the elements," Phil. Mag. **26**, 1024 (1913); **27**, 703 (1914).

[12] C. F. von Weizsäcker, "Zur Theorie der Kernmassen," Z. Phys. **96**, 431 (1935).

[13] P. Cappellaro, *Introduction to Applied Nuclear Physics* (MIT OpenCourseWare / LibreTexts), CC BY-NC-SA 4.0.

[14] J.-L. Basdevant, J. Rich, and M. Spiro, *Fundamentals in Nuclear Physics: From Nuclear Structure to Cosmology*, Springer, New York (2005).

[15] D. Tong, *Particle Physics*, Lecture notes (University of Cambridge / CERN school notes).

[16] M. G. Mayer, "On closed shells in nuclei. II," Phys. Rev. **75**, 1969 (1949).

[17] O. Haxel, J. H. D. Jensen, and H. E. Suess, "On the "magic numbers" in nuclear structure," Phys. Rev. **75**, 1766 (1949).

[18] T. Schmidt, "Über die magnetischen Momente der Atomkerne," Z. Phys. **106**, 358 (1937).

[19] L. W. Nordheim, "On spins, moments, and shells in nuclei," Phys. Rev. **78**, 294 (1950).

[20] Evaluated Nuclear Structure Data File (ENSDF), National Nuclear Data Center, Brookhaven National Laboratory, `https://www.nndc.bnl.gov/ensdf/`.

[21] NuDat 3, National Nuclear Data Center, Brookhaven National Laboratory, `https://www.nndc.bnl.gov/nudat3/`.

[22] N. J. Stone, "Table of nuclear magnetic dipole and electric quadrupole moments," At. Data Nucl. Data Tables **90**, 75 (2005); updated compilations at NNDC.

[23] W. N. Cottingham and D. A. Greenwood, *An Introduction to Nuclear Physics* (2nd ed.), Cambridge University Press, Cambridge (2001).

[24] H. Geiger and J. M. Nuttall, "The ranges of the α particles from the radioactive substances," Phil. Mag. **22**, 613 (1911).

[25] G. Gamow, "Zur Quantentheorie des Atomkernes," Z. Phys. **51**, 204 (1928).

[26] R. W. Gurney and E. U. Condon, "Wave mechanics and radioactive disintegration," Nature **122**, 439 (1928); Phys. Rev. **33**, 127 (1929).

[27] M. Wang, W. J. Huang, F. G. Kondev, G. Audi, and S. Naimi, "The AME 2020 atomic mass evaluation (II). Tables, graphs and references," Chin. Phys. C **45**, 030003 (2021).

[28] Laboratoire National Henri Becquerel (LNHB), Recommended decay data, `http://www.lnhb.fr/nuclear-data/nuclear-data-table/`.

[29] L. M. Langer, R. D. Moffat, and H. C. Price, Jr., "Low energy beta-ray spectra: P^{32} and Cu^{64}," Phys. Rev. **76**, 1725 (1949).

[30] L. M. Langer and H. C. Price, Jr., "Shapes of the beta-spectra of the forbidden transitions of Sb^{124}, Rb^{86}, Sr^{89}, Y^{91}, and Cs^{137}," Phys. Rev. **75**, 1769 (1949).

[31] D. C. Camp and L. M. Langer, "The shape of the ^{66}Ga positron spectrum and the contribution from $0^+ \to 0^+$ transitions," Phys. Rev. **129**, 1782 (1963).

[32] H. C. Verma, *Nuclear Physics: Fundamentals and Applications*, NPTEL/IIT Kanpur lecture series, `https://hcverma.in/ncl_phy_lectures`.

[33] International Atomic Energy Agency, *LiveChart of Nuclides*, evaluated structure, decay, reaction, and fission-yield data, `https://www-nds.iaea.org/relnsd/vcharthtml/VChartHTML.html`.

[34] T. Kibédi, T. W. Burrows, M. B. Trzhaskovskaya, P. M. Davidson, and C. W. Nestor, Jr., "Evaluation of theoretical conversion coefficients using BrIcc," Nucl. Instrum. Methods Phys. Res. A **589**, 202 (2008), DOI: 10.1016/j.nima.2008.02.051.

[35] D. A. Brown *et al.*, "ENDF/B-VIII.0: The 8th major release of the nuclear reaction data library with CIELO-project cross sections, new standards and thermal scattering data," Nucl. Data Sheets **148**, 1 (2018), DOI: 10.1016/j.nds.2018.02.001.

[36] B. Acharya *et al.*, "Solar fusion III: New data and theory for hydrogen-burning stars," Rev. Mod. Phys. **97**, 035002 (2025), DOI: 10.1103/8lm7-gs18.

[37] S. N. Ghoshal, "An experimental verification of the theory of compound nucleus," Phys. Rev. **80**, 939 (1950), DOI: 10.1103/PhysRev.80.939.

[38] D. Adhikari *et al.* (PREX Collaboration), "Accurate determination of the neutron skin thickness of ^{208}Pb through parity-violation in electron scattering," Phys. Rev. Lett. **126**, 172502 (2021), DOI: 10.1103/PhysRevLett.126.172502.

[39] B. T. Reed, F. J. Fattoyev, C. J. Horowitz, and J. Piekarewicz, "Implications of PREX-II on the equation of state of neutron-rich matter," Phys. Rev. Lett. **126**, 172503 (2021), DOI: 10.1103/PhysRevLett.126.172503.

[40] B. Hu *et al.*, "Ab initio predictions link the neutron skin of ^{208}Pb to nuclear forces," Nature Phys. **18**, 1196 (2022), DOI: 10.1038/s41567-022-01715-8.

[41] E. Epelbaum, H.-W. Hammer, and U.-G. Meißner, "Modern theory of nuclear forces," Rev. Mod. Phys. **81**, 1773 (2009), DOI: 10.1103/RevModPhys.81.1773.

[42] H.-W. Hammer, S. König, and U. van Kolck, "Nuclear effective field theory: Status and perspectives," Rev. Mod. Phys. **92**, 025004 (2020), DOI: 10.1103/RevModPhys.92.025004.

[43] T. Otsuka, A. Gade, O. Sorlin, T. Suzuki, and Y. Utsuno, "Evolution of shell structure in exotic nuclei," Rev. Mod. Phys. **92**, 015002 (2020), DOI: 10.1103/RevModPhys.92.015002.

[44] H. Hergert, S. K. Bogner, T. D. Morris, A. Schwenk, and K. Tsukiyama, "The in-medium similarity renormalization group: A novel ab initio method for nuclei," Phys. Rep. **621**, 165 (2016), DOI: 10.1016/j.physrep.2015.12.007.

[45] J. M. Lattimer and M. Prakash, "The equation of state of hot, dense matter and neutron stars," Phys. Rep. **621**, 127 (2016), DOI: 10.1016/j.physrep.2015.12.005.

[46] J. M. Lattimer, "Neutron stars and the nuclear matter equation of state," Annu. Rev. Nucl. Part. Sci. **71**, 433 (2021), DOI: 10.1146/annurev-nucl-102419-124827.

[47] B. P. Abbott *et al.* (LIGO Scientific Collaboration and Virgo Collaboration), "GW170817: Observation of gravitational waves from a binary neutron star inspiral," Phys. Rev. Lett. **119**, 161101 (2017), DOI: 10.1103/PhysRevLett.119.161101.

[48] M. J. Dolinski, A. W. P. Poon, and W. Rodejohann, “Neutrinoless double-beta decay: Status and prospects,” Annu. Rev. Nucl. Part. Sci. **69**, 219 (2019), DOI: 10.1146/annurev-nucl-101918-023407.

[49] M. Agostini, G. Benato, J. A. Detwiler, J. Menéndez, and F. Vissani, “Toward the discovery of matter creation with neutrinoless $\beta\beta$ decay,” Rev. Mod. Phys. **95**, 025002 (2023), DOI: 10.1103/RevModPhys.95.025002.

[50] P. Gysbers *et al.*, “Discrepancy between experimental and theoretical β-decay rates resolved from first principles,” Nature Phys. **15**, 428 (2019), DOI: 10.1038/s41567-019-0450-7.

[51] H. L. Crawford, K. Fossez, S. König, and A. Spyrou, “A vision for the science of rare isotopes,” Annu. Rev. Nucl. Part. Sci. **74**, 141 (2024), DOI: 10.1146/annurev-nucl-121423-091501.

[52] Nuclear Science Advisory Committee, *A New Era of Discovery: The 2023 Long Range Plan for Nuclear Science*, U.S. Department of Energy and National Science Foundation (2023), `https://nuclearsciencefuture.org/`.

[53] S. A. Giuliani, Z. Matheson, W. Nazarewicz, E. Olsen, P.-G. Reinhard, J. Sadhukhan, B. Schuetrumpf, N. Schunck, and P. Schwerdtfeger, “Colloquium: Superheavy elements: Oganesson and beyond,” Rev. Mod. Phys. **91**, 011001 (2019), DOI: 10.1103/RevModPhys.91.011001.

[54] N. Schunck and D. Regnier, “Theory of nuclear fission,” Prog. Part. Nucl. Phys. **125**, 103963 (2022), DOI: 10.1016/j.ppnp.2022.103963.

[55] I. Counts, J. Hur, D. P. L. Aude Craik, H. Jeon, C. Leung, J. C. Berengut, A. Geddes, A. Kawasaki, W. Jhe, and V. Vuletić, “Evidence for nonlinear isotope shift in Yb^+ search for new boson,” Phys. Rev. Lett. **125**, 123002 (2020), DOI: 10.1103/PhysRevLett.125.123002.

[56] I. Angeli and K. P. Marinova, “Table of experimental nuclear ground state charge radii: An update,” At. Data Nucl. Data Tables **99**, 69 (2013), DOI: 10.1016/j.adt.2011.12.006.

[57] S. Kraemer *et al.*, “Observation of the radiative decay of the ^{229}Th nuclear clock isomer,” Nature **617**, 706 (2023), DOI: 10.1038/s41586-023-05894-z.